Modeling of Ultrasonic Processing

Margaret Roylance, John Player, Walter Zukas,* David Roylance†

Foster-Miller Inc., Waltham, Massachusetts

Received 11 November 2003; accepted 21 December 2003
DOI 10.1002/app.20595
Published online in Wiley InterScience (www.interscience.wiley.com).

ABSTRACT: Curing of fiber-reinforced thermoset polymer composites requires an elevated temperature to accelerate the crosslinking reaction and also hydrostatic pressure to consolidate the part and suppress the formation of voids. These processing conditions can be provided by autoclaves of appropriate size, but these are expensive and sometimes difficult to schedule. Ultrasonic debulking followed by oven cure is an attractive alternative to autoclave cure. In this technique a movable "horn" driven at ultrasonic frequency is applied to the surface of the uncured part. This generates pressure and at the same time produces heating by viscoelastic dissipation. The part can be debulked to net shape and staged through the action of the ultrasound. There are a large enough number of experimental parameters in ultrasonic debulking and staging to make purely empirical process optimization difficult, and this paper outlines numerical simulation methods useful in understanding and developing the process. © 2004 Wiley Periodicals, Inc. J Appl Polym Sci 93: 1609–1615, 2004

Key words: composites; computer modeling; curing of polymers; differential scanning calorimetry (DSC); viscoelastic properties

INTRODUCTION

Ultrasonic tape lamination (UTL) is a technique that uses high-frequency loading to achieve heating and consolidation of fiber-reinforced composite materials via viscoelastic energy dissipation.[1] In conjunction with E-Beam curing or a variety of thermal techniques, such as solid state cure, UTL provides an avenue for out-of-autoclave curing of high-quality, large-scale fiber placed composite structures. This approach offers the possibility of out-of-autoclave processing without the development and qualification of new resin formulations.

Although the use of ultrasonic welding of metals and unreinforced polymeric materials is an important industrial process, process innovations have only recently made the use of ultrasound for the consolidation of polymer matrix composites containing more than 35 to 40% by volume of reinforcing fiber possible. Among other process parameters, experiments have demonstrated that the angle at which insonification occurs is a critical process variable. Figure 1 shows the UTL head mounted on a filament winder. To induce consolidation without damaging a fiber-reinforced composite, a horn angle of less than 90° is required. Changing the horn angle changes the stress state in the material during insonification and thus changes the relative amount of energy dissipated by viscoelastic heating of the matrix compared to fiber disruption.

Experiments have shown UTL to be effective both for consolidation of thermoplastic matrix composite materials and debulking of B-staged thermoset prepreg.[2] In both processes the ultrasonic loading must generate sufficient heat to induce flow and provide sufficient support for consolidation, but one added complication of UTL of thermosets is the potential for thermally induced curing. An ability to model and control this chemical reaction is essential to the use of UTL as part of an out-of-autoclave processing scheme. This paper will describe some of the development required for such a model, and some examples of the results that can be obtained from it.

To clarify the relative importance of frictional and viscoelastic heating, the effects of pressure and amplitude on UTL-induced heating have been measured.[3] The data showed that increasing the static pressure has no observable effect on the heat generation in the material during UTL, suggesting that the viscoelastic heating is dominating the UTL heat generation. This conclusion is in agreement with the results of Tolunay et al.,[4] which showed, for soft polymers, the interface did not have a significant effect on the amount of heat dissipated during ultrasonic welding of unreinforced materials. They observed that in this case the heating occurs over the whole volume.

Correspondence to: D. Roylance (roylance@mit.edu).
*Permanent address: W. Zukas, U.S Army Soldier and Biological Chemical Command, Natick, MA.
†Permanent address: Department of Materials Science and Engineering, Massachusetts Institute of Technology, Cambridge, MA 02139.

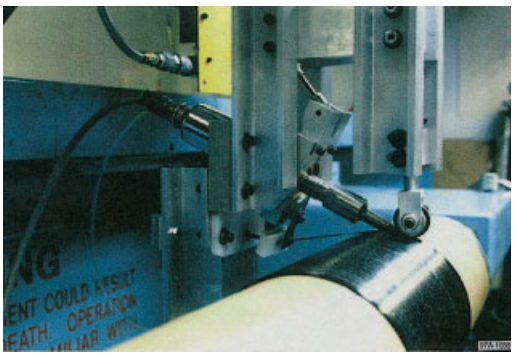

Figure 1 Ultrasonic tape lamination during filament winding.

Further, they observed that intensive heating of the material began only after a certain temperature was reached. This temperature most probably corresponds to the glass transition temperature, since, as T_g is approached, the level of viscoelastic energy dissipation as measured by loss modulus increases markedly. As the material continues to heat above T_g, the loss modulus drops again, and Tolunay et al.[4] observed that the heating rate also generally drops until the temperature remains constant. Based on these results, the UTL process model described here focuses on viscoelastic energy dissipation and reaction exotherm as volumetric heat sources rather than frictional heating at the interfaces.

VISCOELASTIC DISSIPATION OF UNCURED RESIN

A first step in developing a process model for ultrasonic consolidation is estimating the amount of thermal energy dissipated during a loading cycle. This can be written in terms of the material's "loss" modulus E'' in the theory of linear viscoelasticity.[5] The material's complex modulus $E^* = E' + iE''$ is a function of both temperature and frequency, and a convenient model for this dependency is the "Wiechert" viscoelastic expression

$$E' = k_0 + \sum_{j=1}^{N} \frac{k_j(\omega\tau_j)^2}{1 + (\omega\tau_j)^2}, \qquad E'' = \sum_{j=1}^{N} \frac{k_j(\omega\tau_j)}{1 + (\omega\tau_j)^2} \quad (1)$$

where the k's and τ's are adjustable constants and $\omega = 2\pi f$ is the frequency (rad/s). The Wiechert model can be represented by a spring-dashpot analogy, with the k's being spring stiffnesses and the τ's being associated relaxation times. The temperature dependence is introduced by making the τ's an Arrhenius expression of the form

$$\tau_j = \tau_{0j}\exp\left(\frac{E'}{R_g T}\right) \quad (2)$$

where the τ_{0j} are preexponential constants and E^τ is an activation energy for viscoelasticity. Each τ_j is given the same activation energy, which renders the model "thermorheologically simple" and amenable to time–temperature shifting methodology.

Numerical parameters for this model have been obtained by means of dynamic mechanical analyses (DMA) of uncured prepreg in which an oscillatory load was applied to the surface of the prepreg lay-up. The prepreg utilized in this study was a unidirectional IM7 fiber tow impregnated with Hexcel Corp.'s 8552 thermoplastic-toughened high-performance epoxy resin. The prepreg was stored in a freezer at –30°C until used. Plies were layered in a 0/90 configuration for DMA using a Perkin–Elmer DMA 7e, set up for dynamic compression experiments between parallel plates. The frequency was scanned from approximately 1 to 30 Hz under isothermal conditions, and the experiment was repeated at various temperatures from 5 to 60°C.

The data at various temperatures could be superimposed by horizontal shifting along the frequency axis. The temperature dependence of the shift parameter can be used to compute the activation energy E^τ for the process, as well. Equation 2 implies that a plot of the logarithm of the shift factor versus inverse temperature will appear as a straight line of slope E^τ/R_g. The Arrhenius plot for the DMA data is shown in Figure 2, and the line slope gives $E^\tau = 69.1$ kJ/mol.

The shifted master curve for the storage modulus E' versus cyclic frequency is shown in Figure 3, along with the model fit of eqs. (1) and (2).

The same model parameters used in the fit to the storage modulus in Figure 3 can be used in modeling the loss modulus E'', as shown in Figure 4. The experimental DMA data for E'' do not shift as smoothly as those for the storage modulus, but they suffice to show the reasonableness of the model fit.

The analytical model can be used to predict any desired viscoelastic function (relaxation, creep, ran-

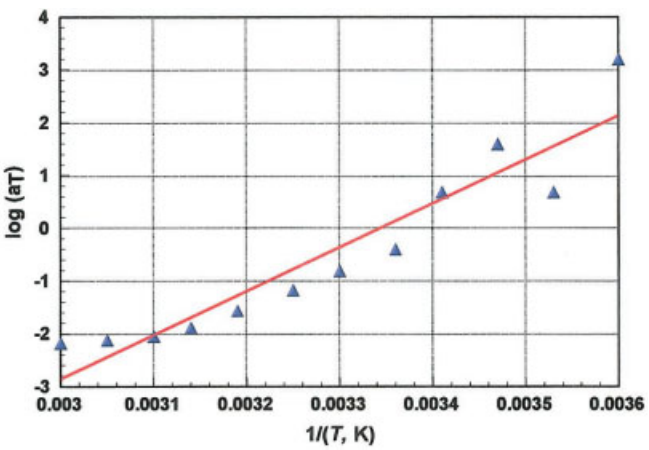

Figure 2 Arrhenius plot of viscoelastic shift factors.

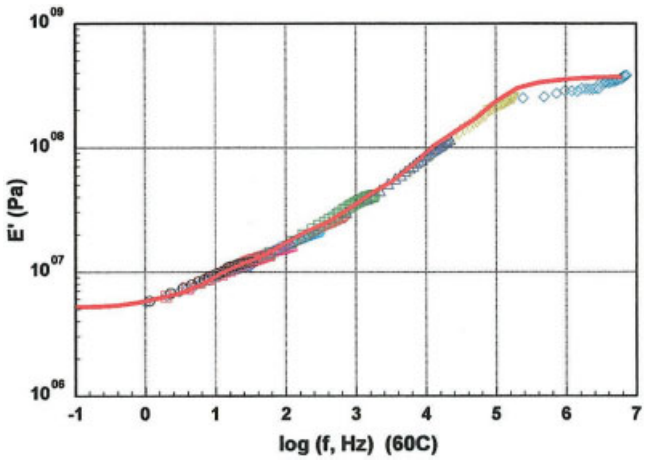

Figure 3 Experimental (with different symbol shapes indicating temperature) and model analysis (solid line) of 8552 storage modulus.

dom loading, etc.) or to plot versus temperature as well as time or frequency. In particular, the model provides a means of extrapolating the viscoelastic dissipation from the low frequencies of the DMA characterization to the higher ultrasonic frequencies used in actual processing. Figure 5 below shows the loss modulus at 40 kHz, plotted against temperature. These data show a high-frequency glass transition (the peak of the loss modulus) occurring at approximately 50°C.

KINETICS OF CURE

The 8552 epoxy formulation cures via rearrangement of the epoxide group on the resin and amine hydrogen on the hardener (Fig. 6).

The reaction rate might be expected to vary with the concentration of reactant and for equal stoichiometric mixtures of resin and hardener this would lead to a factor proportional to $(1 - \alpha)$,[2] where $\alpha = C/C_0$ is the extent of reaction and C and C_0 are the current and

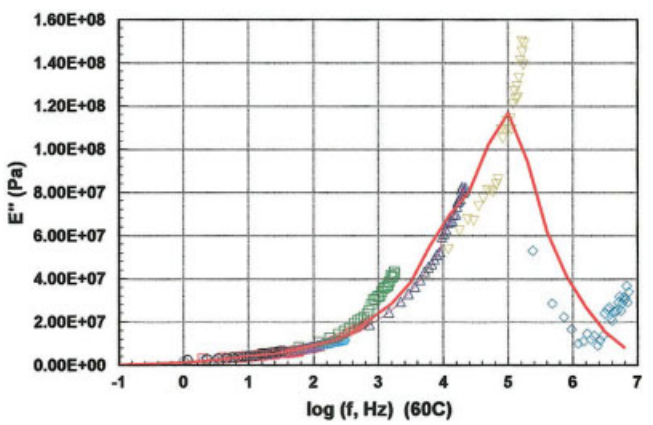

Figure 4 Experimental (different symbol shapes indicating temperature) and model analysis of 8552 loss modulus.

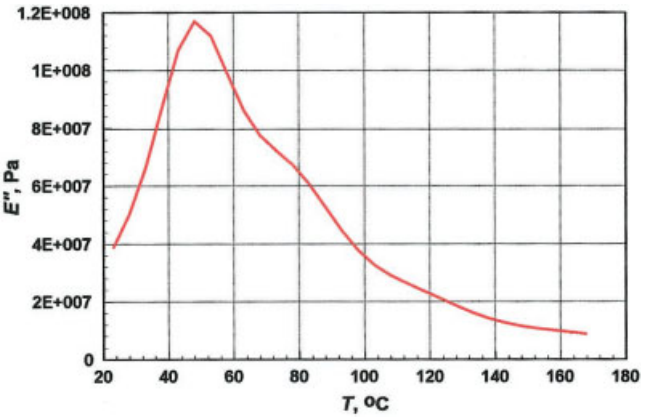

Figure 5 Model prediction of temperature dependence of 40 kHz loss modulus E''.

initial concentration of reactants. In addition, the reaction is autocatalyzed by hydroxyl groups that are generated by the epoxide rearrangement. This produces an additional factor of α in the kinetic relation. Using an Arrhenius relation for the temperature dependence of the rate, we can propose a simple kinetic relation of the form

$$\frac{d\alpha}{dt} = k_0 \exp\left(\frac{-E^r}{R_g T}\right) \times \alpha^{m1}(1-\alpha)^{m2} \qquad (3)$$

where k_0 is a preexponential constant, E^r is an activation energy for reaction, and $R_g = 8.314$ J/mol-°K is the gas constant. We allow the kinetic order exponents on the concentration factors to be $m1$ and $m2$ rather than 1 and 2; this permits needed flexibility in the ability of this convenient but simple model to fit experimental data.

The kinetic constants in the cure relation were chosen to fit calorimetic (differential scanning calorimetry, DSC) data obtained by Ng et al.[6] for the 8552

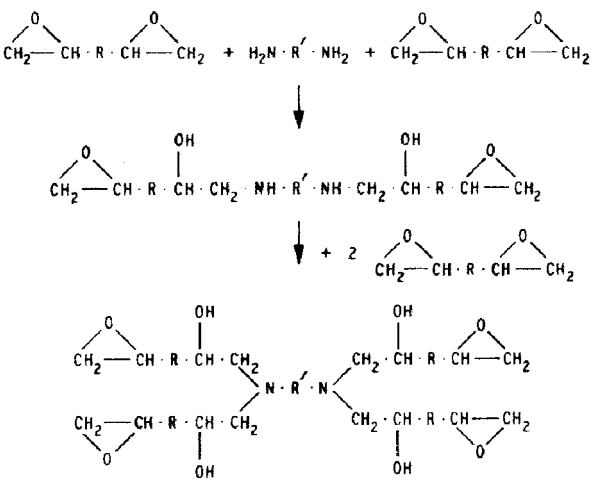

Figure 6 Generic reaction mechanism for epoxy–amine cure.

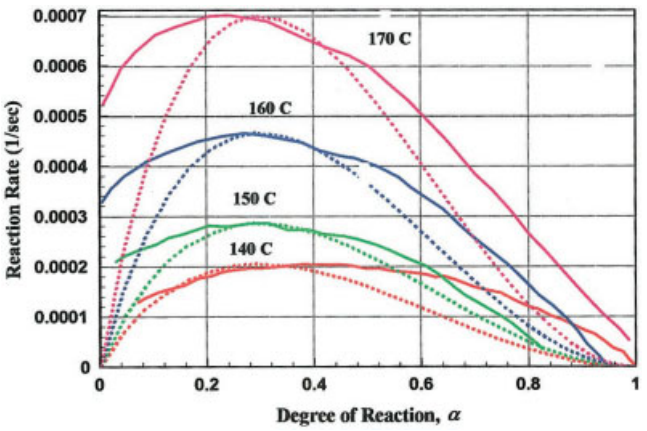

Figure 7 Calorimetric (solid lines) and model (dotted lines) analysis of 8552 cure kinetics.

epoxy. These experimental data, indicated by solid lines in Figure 7, are plotted to show reaction rate as a function of degree of cure. Note that the rate rises initially as the hydroxyl concentration increases, and eventually falls as the epoxide and hardener are consumed. The dotted lines show the prediction of the kinetic cure model [eq. (3)[rsqb], with the parameters: $k_0 = 1.27 \times 10^5$ s^{-1}, $E^r = 63.4$ kJ/mol, $m1 = 0.9$, $m2 = 2.1$). The DSC studies also gave the total heat of reaction as $\Delta H = 483$ J/g.

The kinetic model of eq. (3) can be used in assessing and optimizing resin cure cycles and can predict when gelation and vitrification occur during cure. As the crosslinking reaction proceeds, eventually some molecules will reach degrees of polymerization approaching infinity. This onset of an infinite molecular network, and the degree of reaction corresponding to this state, is termed the "gel point." Gelation is a vitally important transformation in processing, marking the transition from a liquid to a solid. Once the resin has gelled it is no longer processable, and operations such as layup and void removal are no longer possible.

Gelation is associated with a fixed degree of reaction, calculable from statistical theory. The Carouthers Equation is a simple example of gelation theory and can be stated as[7]

$$\alpha_{gel} = \frac{2}{f_{avg}} \tag{4}$$

where α_{gel} is the extent of reaction at which gelation occurs, and f_{avg} is the average functionality of the system. For a difunctional resin ($f = 2$) and a tetrafunctional hardener ($f = 4$), we have $f_{avg} = 3$ and $\alpha_{gel} = 0.67$.

Crosslinking also inhibits molecular mobility and with increasing cure the glass transition temperature T_g increases from the value corresponding to a completely uncured resin T_{g0} to that of the fully cured system $T_{g\infty}$. The value of T_g is a direct function of the extent of reaction α, which the DiBenedetto Equation states as[8]

$$T_g = \frac{(1-\alpha)T_{g0} + \lambda\alpha T_{g\infty}}{(1-\alpha) + \lambda\alpha} \tag{5}$$

Thermodynamic reasoning gives the parameter λ as the ratio $\Delta c_{p\infty}/\Delta c_{p0}$, where the Δc_p values are the differences between the specific heats in the rubbery and glassy states for the fully cured and fully uncured resin, respectively.

The kinetic model of eq. (3) can be solved numerically to compute the degree of cure at various times in an isothermal cure process, with a specimen size small enough to neglect spatial variation. The time to gelation is observed as that at which the extent of cure reaches the gel point as given by eq. (4), and the time to vitrification is that at which the T_g which rises above the cure temperature. In Figure 8 the times to

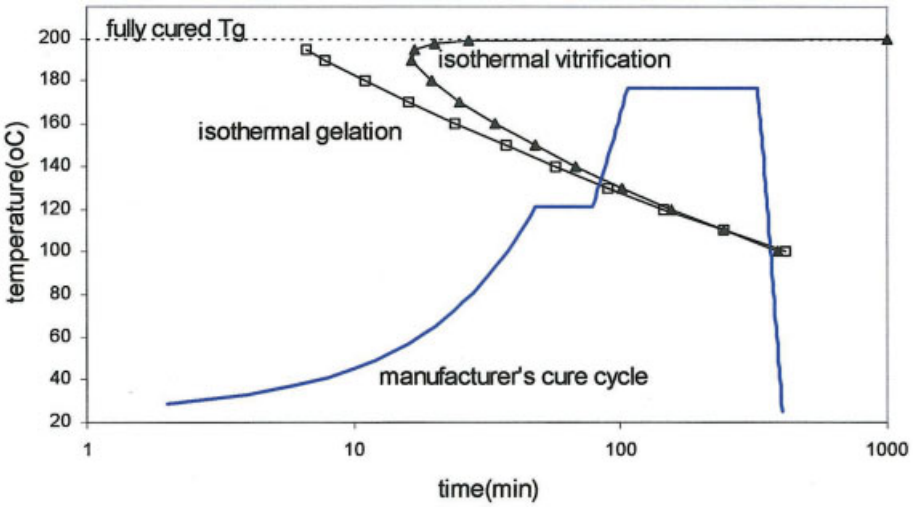

Figure 8 Predicted isothermal TTT diagram for 8552 and comparison with manufacturer's (nonisothermal) cure cycle.

gelation and vitrification are plotted against the (isothermal) cure temperature, giving the "TTT" diagram popularized by Gillham and Enns[9] The manufacturer's suggested cure program (obviously nonisothermal) is plotted on this figure as well; this is in the spirit of the common practice of drawing cooling curves on metallurgical TTT diagrams, but the inconsistency of putting isothermal and nonisothermal curves on the same graph should be kept in mind. Even so, it permits an estimate of the cure state during the cycle.

As expected, the times to both gelation and vitrification become longer at lower cure temperatures. However, as discussed by Gillham and Enns,[9] the vitrification curve must bend to longer times, approaching infinity, as the cure temperature exceeds $T_{g\infty}$, since above this temperature even the fully cured system will be rubbery.

When the resin vitrifies, the reaction is strongly quenched, so at cure temperatures below the crossing point of the gelation and vitrification curves (approximately 75°C in Fig. 8) the gelation curve becomes largely horizontal. This temperature is called ${}_{\text{gel}}T_{\text{g}}$ by Gillham and Enns[9] and denotes the maximum safe storage temperature for the resin. At temperatures below this, the resin will never gel, since vitrification occurs first and quenches further crosslinking. (Prudence dictates that unreacted resin should be stored in a freezer until used, however.)

The quenching effect can be modeled, if desired. When T_g becomes greater than the current curing temperature, the reaction rate equation [eq. (3)[rsqb] can be modified according to Kaeble[10] by replacing the preexponenetial constant k_0 as follows:

$$\ln k_0(T) = \ln k_0(T_g) + \frac{40.7(T - T_g)}{51.6 + (T - T_g)} \tag{6}$$

where $k_0(T_g)$ is the frequency factor at T_g and is assumed to have the same value as in the rubbery or liquid state. The second term is a WLF-type expression that attempts to account for the reduced free volume and molecular mobility at temperature below T_g. This extension to the model does allow crosslinking to proceed, albeit at a much reduced rate, even when the T_g becomes greater than the curing temperature. This results in the $T_{g\infty}$ of the 8552 resin being higher ($T_{g\infty}$ = 200°C) than the upper curing temperature (177°C).

ULTRASONIC LOADING MODEL

During cyclic loading of a viscoelastic material, a fraction of the mechanical energy imparted to the material is dissipated as heat. The heat generation rate (J/m^3-s) is given by[5]

$$Q = f \times \pi E'' \varepsilon_0^2 \tag{7}$$

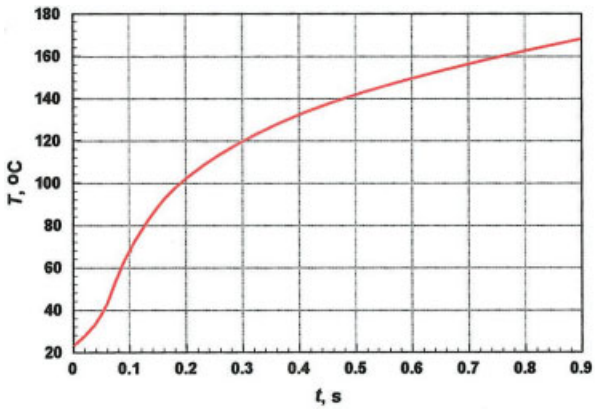

Figure 9 Spreadsheet model prediction of temperature history in carbon/8552 composite cycled at 1.4% strain at 40 kHz.

where f is the frequency (Hz), E'' is the loss modulus (Pa), and ε_0 is the strain amplitude. This heat generation produces a temperature increase in the absence of heat transfer at a rate

$$\frac{dT}{dt} = \frac{Q}{\rho c} \tag{8}$$

where ρ is the density (kg/m^3) and c is the specific heat (J/kg-°C).

These relations have been incorporated into a simple spreadsheet model that operates in a stepwise fashion by starting at room temperature (or any desired starting temperature) and computing the corresponding reaction rate from eq. (3) and the loss modulus from eqs. (1) and (2). The heating rate Q is then computed from eq. (7), along with a contribution from reaction heating given by $\dot{\alpha} \times \Delta H$. The rate of temperature increase is then computed from eq. (8), and a time step corresponding to a moderate temperature increase (say 5°C) is computed from the heating rate. A new temperature and time are computed from these values, and the process repeated on the next row of the spreadsheet.

Even though the spreadsheet does not model the spatial variation of the actual process, it is extremely simple to operate and is thus useful in exploring parameter significance and debugging more advanced models. Figure 9 below shows the temperature history of a graphite/8552 composite loaded at 40 kHz, which shows that the temperature levels off once the material is hot enough to bring the loss modulus to low values as shown in Figure 5. At this cyclic loading rate the heating is very rapid, reaching temperatures over 160°C in less than a second. The reaction rate [eq. (3)[rsqb] is on the order of 10^{-4} at these temperatures, so negligible curing occurs during the ultrasonic loading. Ultrasonic loading of this particular resin thus produces consolidation rather than cure. Suitable modifications of resin chemistry and loading param-

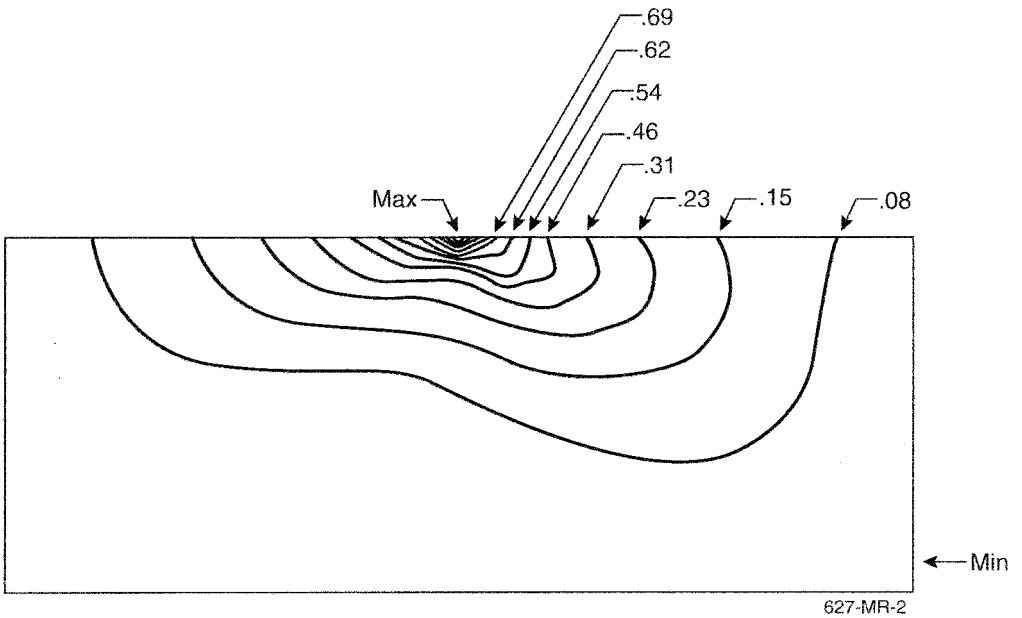

Figure 10 Initial contours of constant horizontal displacement u_x due to isonification at 30 deg.

eters, however, could make ultrasonic loading a method for either cure or consolidation, or both.

There are many experimental parameters in ultrasonic heating not included in the spatially uniform model describe above, including horn angle, contact pressure, frequency and amplitude, presence of attenuating layers, and others. This makes optimization by purely experimental trials difficult and time consuming, and more elaborate computer modeling is useful in this regard. Since commercial finite element analysis (FEA) codes do not always have the particular mix of features needed in a given task, we have used a code adapted from the Zienkiewicz[11] text, with a special element developed by Roylance et al.[12] to model nonisothermal reactive processing operations. Benetar and Gutowski[13] have used this element to predict the behavior of AS4/PEEK during attempted ultrasonic welding using energy directors.

The element in our FEA code models the equations governing the nonisothermal flow of a reactive fluids, listed in standard texts on transport phenomena and polymer processing (e.g., references 14 and 15). These are the familiar conservation equations for transport of momentum, energy, and species:

$$\begin{aligned} \rho\left[\frac{\partial u}{\partial t} + u\nabla u\right] &= -\nabla p + \nabla(\eta\nabla u) \\ \rho c\left[\frac{\partial T}{\partial t} + u\nabla T\right] &= Q + \nabla(k\nabla T) \\ \left[\frac{\partial C}{\partial t} + u\partial C\right] &= R + \nabla(D\nabla C) \end{aligned} \tag{9}$$

Here u, T, and C are fluid velocity (a vector), temperature, and concentration of reactive species; these are the principal variables in our formulation. Other parameters are density (ρ), pressure (p), viscosity (η), specific heat (c), thermal conductivity (k), and species diffusivity (D). The ∇ operator is defined as $\nabla = \partial/\partial x, \partial/\partial y$.

Q and R are generation terms for heat and chemical species, respectively, while the pressure gradient ∇p plays an analogous role for momentum generation. The heat generation arises from viscous dissipation and from reaction heating:

$$Q = \tau{:}\dot{\gamma} + R(\Delta H)$$

where τ and $\dot{\gamma}$ are the deviatoric components of stress and strain rate, R is the rate of chemical reaction, and ΔH is the heat of reaction.

In treating ultrasonic curing, we take the velocities u in the governing equations to be displacements and suppress the advective flow terms (e.g., $u\nabla u$). In this approach, the dilatational and deviatoric components of stress are considered separately, which leads to convenience in handling incompressible materials. It also simplifies the computation of internal dissipative heating, which arises principally from the deviatoric components of stress. The viscous dissipation heating is computed as in eq. (7).

The analysis operates in iterative fashion, first solving the force equilibrium equations to determine the distribution of displacement, strain, and stress generated in the body by the application of the imposed displacements at the surface. This heat dissipation associated with the viscous loss is used in the heat transfer equation, which is solved for an updated estimate of the temperature in a second iteration. In a third iteration the temperatures obtained in the previous step are used to update the rate of the chemical

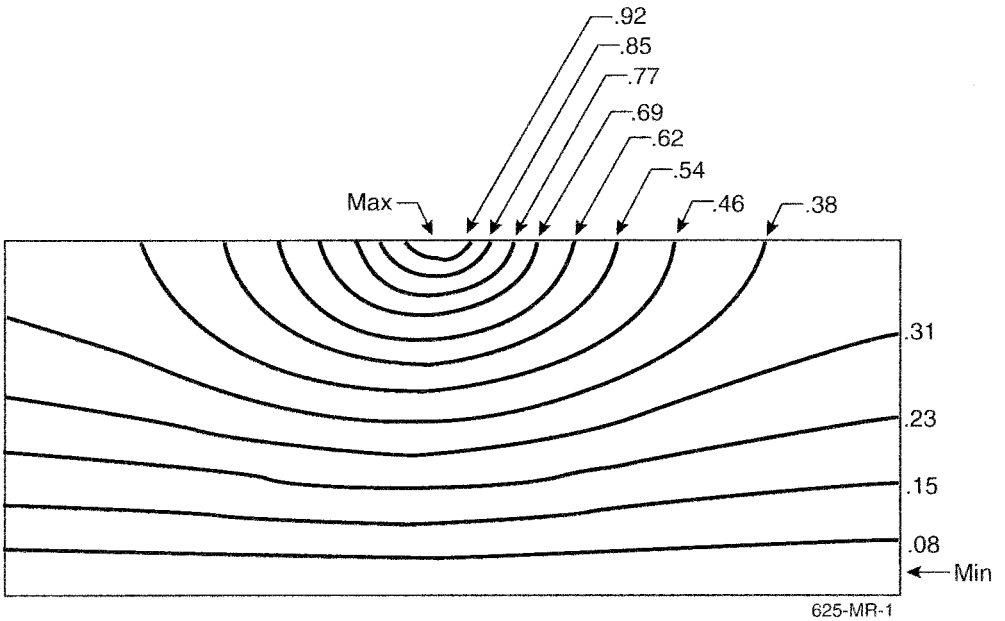

Figure 11 Temperature field arising from the displacements of Figure 7.

curing reaction. The equations are strongly coupled, with properties such as the shear modulus and chemical reaction rate depending on temperature, and the temperature depending on both viscous and reaction heating. The computer iterates repeatedly until convergence is reached. The code can also use successive iterations as time steps, so that transient situations can be modeled as well.

Figure 10 shows the initial contours of constant horizontal displacement generated by the FEA code by an ultrasonic displacement applied to the surface of a two-ply laminate at 30° from the horizontal. This is basically the displacement field of an elastic point-contact problem, with asymmetry arising from the oblique direction of application of the ultrasonic horn.

The displacements imposed by the ultrasonic horn are concentrated near the point of application, so the heat generation rate is highest here. However, heat will also be carried to other regions of the specimen by conduction. The temperature field arising from this oscillatory stress field is shown in Figure 11.

CONCLUSION

Several conclusions may be drawn from the results of the model development to date:

- The viscoelastic properties of the prepreg material at loading rates in the 20 to 40 kHz range are difficult to measure directly, and development of techniques to predict this response are critical to the UTL model.
- The dynamic response of the 8552 resin appears to obey time–temperature superposition to a reasonable extent, and it is possible to use shifting to obtain a frequency- and temperature-dependent viscoelastic characterization.
- The cure kinetics model used in this work provides a good fit to the experimental curing data for 8552.
- Insonification can induce very rapid localized heating. Temperatures well above the standard cure temperature can be achieved in seconds, but advancement of the cure may be slight.
- Once the ability of the model to predict heating and staging induced by a stationary ultrasonic horn is established, the analysis should be extended to predict the effects of horn motion

References

1. Branson Ultrasonic Corporation. Ultrasonic Plastics Assembly, 1979.
2. Benson, V.; Player, J.; Roylance, M. E. Proceedings of the 46th SAMPE Conference, 2001.
3. Roylance, M. E.; Roylance, D. K.; Nesmith, K. L. Proceedings of the 43rd International SAMPE Symposium, 1998.
4. Tolunay, M. N.; Dawson, P. R.; Wang, K. K. Polym Eng Sci 1983, 23, 726.
5. Roylance, D. Mechanics of Materials; Wiley: New York, 1996.
6. Ng, S. J.; Boswell, R.; Claus, S. J.; Arnold, F.; Vizzini, A. J Adv Mater 2002, 34, 33.
7. Young, R. J. Introduction to Polymers; Chapman and Hall: London, 1981.
8. Wisanrakkit, G.; Gillham, J. K. J Appl Polym Sci 1990, 41, 2885.
9. Gillham, J. K.; Enns, J. B. Trends Polym Sci 1983, 2, 406.
10. Kaeble, D. H. In Computer Aided Design and Manufacture; Marcel Dekker: New York, 1985; Chap. 4, pp 113–148.
11. Zienkiewicz, O. C. The Finite Element Method; McGraw-Hill: New York, 1977.
12. Roylance, D.; Chiao, L.; McElroy, P. ACS Symp Ser 1989, 404, 270.
13. Benetar, A.; Gutowski, T. G. SPE Annu Tech Conf 1989, 507.
14. Bird, R. B.; Stewart, W. E.; Lightfoot, E. N. Transport Phenomena; Wiley: New York, 1960.
15. Middleman, S. Fundamentals of Polymer Processing; McGraw-Hill: New York, 1977.